Manipulating superconductivity in ruthenates through Fermi surface engineering

Yi-Ting Hsu,[1] Weejee Cho,[2] Alejandro Federico Rebola,[3] Bulat Burganov,[1] Carolina Adamo,[4,5] Kyle M. Shen,[1,6] Darrell G. Schlom,[4,6] Craig J. Fennie,[3] and Eun-Ah Kim[1]

[1]*Department of Physics, Cornell University, Ithaca, New York 14853, USA*
[2]*Department of Physics, Stanford University, Stanford, California 94305-4060, USA*
[3]*School of Applied and Engineering Physics, Cornell University, Ithaca, New York 14853, USA*
[4]*Department of Materials Science and Engineering, Cornell University, Ithaca, New York 14853, USA*
[5]*Department of Applied Physics, Stanford University, Stanford, California 94305, USA*
[6]*Kavli Institute at Cornell for Nanoscale Science, Ithaca, New York 14853, USA*

(Received 4 May 2016; revised manuscript received 27 June 2016; published 15 July 2016)

The key challenge in superconductivity research is to go beyond the historical mode of discovery-driven research. We put forth a new strategy, which is to combine theoretical developments in the weak-coupling renormalization-group approach with the experimental developments in lattice-strain-driven Fermi surface engineering. For concreteness we theoretically investigate how superconducting tendencies will be affected by strain engineering of ruthenates' Fermi surface. We first demonstrate that our approach qualitatively reproduces recent experiments under uniaxial strain. We then note that the order of a few percent strain, readily accessible to epitaxial thin films, can bring the Fermi surface close to van Hove singularity. Using the experimental observation of the change in the Fermi surface under biaxial epitaxial strain and *ab initio* calculations, we predict T_c for triplet pairing to be maximized by getting close to the van Hove singularities without tuning on to the singularity.

DOI: 10.1103/PhysRevB.94.045118

I. INTRODUCTION

The notion of topological superconductivity [1–7] drove intense investigation of a triplet superconductor Sr_2RuO_4 [8–13]. Unfortunately its fairly low transition temperature $T_c \sim 1.5$ K [14] has been one of the limiting factors for experimental studies. Naturally there has been much interest in enhancing the T_c of Sr_2RuO_4. Since the T_c is extremely sensitive to disorder, the usual tuning knob of doping is not an option. On the other hand, successes in both local enhancement of T_c in eutectic samples [15,16] and near dislocations [17] and in global enhancement of T_c using c-axis uniaxial pressure [18,19] and in-plane uniaxial strain [20] point to a new knob: the lattice strain. Now the key question is how to connect this new knob to a theoretical framework that can guide the quest for a higher-T_c topological superconductor.

T_c is generally hard to theoretically predict since it is a nonuniversal quantity which depends on microscopic details of the system. The fact that one cannot just apply mean-field theory for repulsion-driven anisotropic superconductors makes it even worse. Nevertheless Kohn and Luttinger [21] have observed early on that, even with a short-range bare repulsion, the momentum dependence in the irreducible particle-particle vertex from higher-order corrections can still give rise to a Cooper instability in a suitable channel. This insight was further developed for Hubbard-type models on lattices [22–26]. A common thread in these approaches is the fact that the band structure near Fermi surfaces (FSs) determines the bare susceptibilities which enter the expression for the pairing interaction. This invites the notion of controlling superconductivity through controlling fermiology, going beyond the traditional approach of doping [27–30].

Our idea is to employ the weak-coupling renormalization-group (RG) approach [26,31] in embracing the new experimental knob of lattice strain. Since the pioneering work of Chu *et al.* [32], piezoelectric-based control of lattice strain has become a new knob. This approach was further developed [33] to enable substantial uniaxial strain on bulk Sr_2RuO_4 and led to a 40% enhancement of T_c [20]. A recent experimental advance by some of us in growing epitaxially strained ruthenate films [34] presents a new opportunity. This is particularly exciting because the epitaxial strain can dramatically alter the band structure [34].

Here, we theoretically investigate how strain affects the fermiology and the associated superconducting tendencies. For this, we extract tight-binding parametrization from angle-resolved photoemission spectroscopy (ARPES) data and a density functional theory (DFT) calculation on strained systems. We then use the tight-binding model as the microscopic input for the RG calculation to study superconducting instability. We examine the cases of piezoelectric-based uniaxial strain [20] and epitaxial biaxial strain [34]. We reproduce the observed trend for the case of uniaxial strain and predict nonmonotonic dependence of the T_c on the biaxial strain.

II. THE MODEL AND THE APPROACH

Our microscopic starting point is a three-band Hubbard model derived from the Ru t_{2g} orbitals d_{xz}, d_{yz}, and d_{xy},

$$H = \sum_{\vec{k}\alpha\sigma} \epsilon^{\alpha}(\vec{k}) c^{\dagger}_{\vec{k},\alpha,\sigma} c_{\vec{k},\alpha,\sigma} + U \sum_{i\alpha} n_{i,\alpha,\uparrow} n_{i,\alpha,\downarrow}, \qquad (1)$$

where $\vec{k} = (k_x, k_y)$, $\alpha = xz, yz, xy$, and $\sigma = \uparrow, \downarrow$ denote the crystal momentum, the orbital index, and the spin, respectively, and $n_{i,\alpha,\sigma} \equiv c^{\dagger}_{i,\alpha,\sigma} c_{i,\alpha,\sigma}$. Given the well-established unconventional aspects of superconductivity in bulk Sr_2RuO_4 [8–10], we focus on the repulsive intraorbital on-site repulsion $U > 0$ [21,31,35].

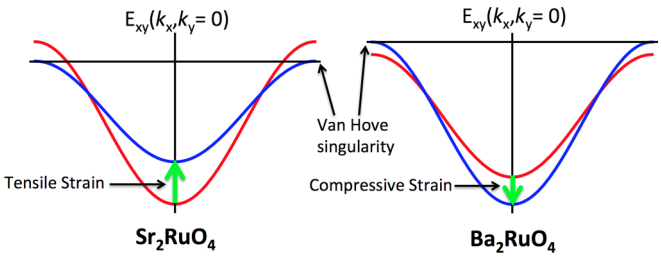

FIG. 1. The effect of epitaxial biaxial strain on the xy 2D band in Sr_2RuO_4 and Ba_2RuO_4, respectively. The red curves are unstrained bands. Bands were obtained by fitting tight-binding parameters to DFT data.

For the intraorbital kinetic energies $\epsilon^{\alpha}(\vec{k})$ we employ the following tight-binding parametrization:

$$\begin{aligned}\epsilon^{xz}(\vec{k}) &= -2t_x \cos\, k_x - 2t_y^{\perp} \cos\, k_y - \mu_1,\\ \epsilon^{yz}(\vec{k}) &= -2t_y \cos\, k_y - 2t_x^{\perp} \cos\, k_x - \mu_1,\\ \epsilon^{xy}(\vec{k}) &= -2(t_x' \cos\, k_x + t_y' \cos\, k_y) - 4t'' \cos\, k_x \cos\, k_y - \mu_2,\end{aligned} \tag{2}$$

where we neglect the orbital-mixing terms. Although Scaffidi *et al.* [36] found the spin-orbit coupling in particular to significantly alter the nature and mechanism of pairing in the unstrained system, the van Hove singularities occur at points $X = (\pi,0)$ and $Y = (0,\pi)$ which lie in the region of the FS where orbital characters are well defined [37–40]. Hence we expect the absence of orbital-mixing terms in our model would not affect our conclusions in a qualitative manner. The dispersions of the three bands in Eq. (2) yield two quasi-one-dimensional (1D) FSs consisting of the Ru orbitals d_{xz} and d_{yz} and one quasi-two-dimensional (2D) FS consisting of the Ru orbital d_{xy}.

We connect the lattice strain to the model Eq. (2) through the ARPES data of Ref. [34] and DFT calculations. Unstrained Sr_2RuO_4 and its close relative Ba_2RuO_4 have van Hove singularities of the d_{xy} character (2D xy band) at the X and Y points slightly above (Sr_2RuO_4) or below (Ba_2RuO_4) the Fermi level (see Appendix B 2). When applying uniaxial tensile strain in the [100] direction on these quasi-2D ruthenates, one expects [20,41] the bandwidth to decrease along the [100] direction while behaving oppositely in the [010] direction. Our DFT calculations indeed predict the density of states of the xz and xy bands to show similar amounts of growth for small magnitudes of uniaxial strain (see Appendix B 1) although it is the xy band that eventually reaches the van Hove singularity at X or Y at a large enough strain (see Appendix B 1). As for the biaxial strain, we predict Sr_2RuO_4 and Ba_2RuO_4 to reach the van Hove singularity at both X and Y points at the Fermi level under a tensile and compressive strain, respectively (see Fig. 1 and Appendix B 2), consistent with the experimental observations of Ref. [34] (see Fig. 3). Moreover, we find this shift to the van Hove singularity to be driven by both the change in the bandwidth of the xy band (see Fig. 1) and the charge transfer from the xz and yz bands (see Appendix A). Nevertheless DFT consistently overestimates the Fermi velocities v_F compared to ARPES, in particular, that of the 2D band xy [34].

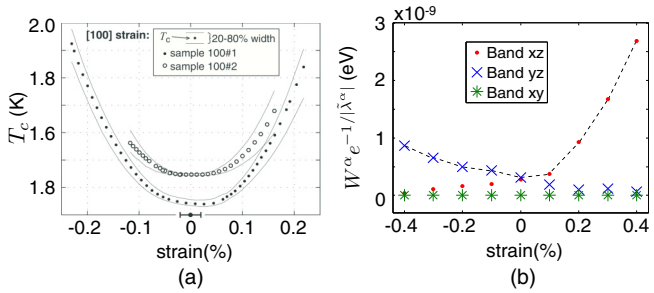

FIG. 2. (a) Measured T_c under both tensile (>0) and compressive (<0) uniaxial strain in the [100] direction presented in Ref. [20]. (b) Calculated quantity $W^{\alpha}e^{-1/|\tilde{\lambda}^{\alpha}|}$ under different amounts of uniaxial strain in the [100] direction with $U = 1$ eV. The black dashed line shows the expected transition temperature T_c.

For completeness we now briefly review the two-step perturbative RG approach [26,31] we adopt. As a first step we numerically calculate the effective pairing vertices in different channels at some intermediate energy scale $E = \Lambda_0$ near the FS by integrating out higher-energy modes down to Λ_0. Up to the one-loop order, the singlet and triplet effective pairing vertices $\Gamma^{\alpha}_{s/t}(\hat{k},\hat{k}')$ at energy Λ_0 are related to the repulsive bare interaction U and the static particle-hole bubbles $\Pi^{\alpha}_{ph}(\vec{q})$ through

$$\Gamma^{\alpha}_{s}(\hat{k},\hat{k}') = U + U^2\Pi^{\alpha}_{ph}(\hat{q} = \hat{k} + \hat{k}'), \tag{3}$$

and

$$\Gamma^{\alpha}_{t}(\hat{k},\hat{k}') = -U^2\Pi^{\alpha}_{ph}(\hat{q} = \hat{k} - \hat{k}'). \tag{4}$$

Now the pairing tendency hosted by band α in each of the two pairing channels can be quantified by the most negative eigenvalue $\tilde{\lambda}^{\alpha}_{s/t} \equiv \lambda^{\alpha}_{s/t}(E = \Lambda_0)$ of a dimensionless matrix $g^{\alpha}_{s/t}(\hat{k},\hat{k}')$, which is a product of the density of states (DOS) $N^{\alpha}(\Lambda_0) \sim N^{\alpha}(0)$ and the normalized effective pairing vertices at the intermediate energy scale Λ_0,

$$g^{\alpha}_{s/t}(\hat{k},\hat{k}') = N^{\alpha}(\Lambda_0)\sqrt{\frac{\bar{v}^{\alpha}_F}{v^{\alpha}_F(\hat{k})}}\Gamma^{\alpha}_{s/t}(\hat{k},\hat{k}')\sqrt{\frac{\bar{v}^{\alpha}_F}{v^{\alpha}_F(\hat{k}')}}. \tag{5}$$

Here $(\hat{k}^{(\prime)})$'s are the outgoing(incoming) momenta on the FS of band α, $v^{\alpha}_F(\hat{k})$ is the magnitude of Fermi velocity at $\hat{k}$, and $\frac{1}{\bar{v}^{\alpha}_F} \equiv \int \frac{d\hat{p}}{S^{\alpha}_F}\frac{1}{v^{\alpha}_F(\hat{p})}$ with $S^{\alpha}_F \equiv \int d\hat{p}$ being the FS "area" of orbital α. The second step is to study the RG flows of the most negative eigenvalues $\lambda^{\alpha}_{s/t}(E)$ for different channels $(\alpha,s/t)$. Given the well-known RG equation for the Cooper instability $\frac{d\lambda^{\alpha}_{s/t}}{dy} = -(\lambda^{\alpha}_{s/t})^2$ in terms of $y \equiv \ln(\Lambda_0/E)$ [42], we can relate T_c to the most negative $\tilde{\lambda}^{\alpha}_{s/t}$'s among all channels $(\tilde{\lambda})$ as $T_c \propto e^{-1/|\tilde{\lambda}|}$ [31].

III. UNIAXIALLY STRAINED Sr_2RuO_4

Hicks *et al.* [20] found the superconducting T_c of Sr_2RuO_4 to enhance under both tensile and compressive uniaxial strain in the [100] direction [see Fig. 2(a)]. They then used phenomenological Ginzburg-Landau analysis to interpret that the enhancement of T_c was driven by the enhancement of density of states in one of the two quasi-one-dimensional

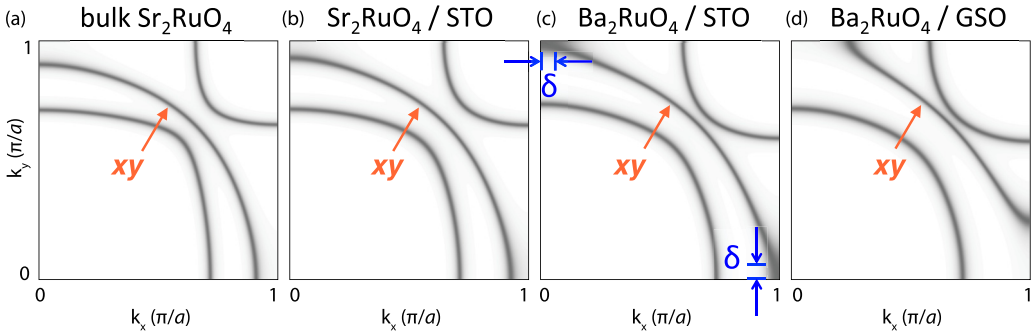

FIG. 3. The spectral functions extracted from the ARPES data in Ref. [34] for (a) the bulk Sr_2RuO_4, (b) Sr_2RuO_4/STO, (c) Ba_2RuO_4/STO, and (d) Ba_2RuO_4/GSO, respectively. The distance from the hole pockets to the van Hove singularities located at $\vec{k} = (\pm\pi, 0)$ and $(0, \pm\pi)$ are denoted by δ in (c). The parametrizations for the bulk Sr_2RuO_4, Sr_2RuO_4/STO, Ba_2RuO_4/STO, and Ba_2RuO_4/GSO are $(t, t^{\perp}, \mu_1, t', t'', \mu_2, t_{hyb}) =$ (0.165,0.0132,0.178,0.119,0.0488,0.176,0.0215), (0.14,0.0126,0.148,0.114,0.0456,0.171,0.0224), (0.115,0.0219,0.112,0.095,0.0365, 0.1463,0.0161), and (0.085, 0.0162, 0.074, 0.07, 0.0245, 0.11, 0.0136) in units of eV, respectively.

bands. Here, by determining the tight-binding parameters from DFT calculations under strain we gain insight into the interplay between strain and electronic structure. By further feeding the strained tight-binding parameters into the RG procedure, we can let our RG flow start from experimentally relevant short-distance physics.

We then carried out the RG analysis to obtain the most negative eigenvalues $\tilde{\lambda}^{\alpha}_{s/t}$, which are determined by the DOS $N^{\alpha}(0)$, bandwidth W^{α}, and the on-site repulsion U. Figure 2(b) shows a quantity corresponding to T_c which involves the pairing tendency of band α quantified by the more negative eigenvalue between singlet and triplet channels $\tilde{\lambda}^{\alpha} \equiv \min(\tilde{\lambda}^{\alpha}_{s}, \tilde{\lambda}^{\alpha}_{t})$ under different amounts of strain. We find that although the strain enhances the density of states of both 1D and 2D bands moderately (see Appendix B 1), the strong pairing interaction of the 1D bands due to the antiferromagnetic fluctuation further amplifies the enhancement in the 1D pairing tendencies $|\tilde{\lambda}^{xz/yz}|$ [43]. As the more dominant of the two 1D bands will onset the superconducting transition, our results imply the transition temperature T_c to follow the dashed curve in Fig. 2(b) as a function of tensile and compressive strain. Note that the estimated value of U from first-principles calculations is on the order of eV [44], which is beyond the weak-coupling regime. Nonetheless, we set $U = 1$ eV in Fig. 2(b) for illustrative purposes. The so-obtained strain dependence of the T_c qualitatively captures the measured trend [20] shown in Fig. 2(b).

IV. BIAXIALLY STRAINED RUTHENATE THIN FILMS

We now turn to the epitaxial ruthenate films under biaxial strain [34]. Biaxial strain has the advantage that it retains the tetragonal symmetry necessary for the onset of the topologically nontrivial $p_x + ip_y$ order parameter. Furthermore, since X and Y points are approached simultaneously the van Hove singularity is expected to have a more substantial impact under biaxial strain (see Appendix B 1 and B 2). On the other hand, epitaxial strain can only access a discrete set of strain values, and likely none will be precisely tuned to the van Hove point. But this may be a blessing since there are two theoretical issues when reaching the van Hove singularity. First, the van Hove points at X and Y points are forbidden from supporting an odd-parity triplet pairing by symmetry [45,46]. Second, other ordering tendencies that can also benefit from the van Hove singularity can compete with superconductivity [47,48]. Hence by being close to a van Hove singularity without tuning into one, epitaxial biaxial strain may optimize triplet pairing.

Four representative samples we consider are the unstrained bulk Sr_2RuO_4, a Sr_2RuO_4 film grown on $SrTiO_3$ (Sr_2RuO_4/STO), a Ba_2RuO_4 film grown on $SrTiO_3$ (Ba_2RuO_4/STO), and a Ba_2RuO_4 film grown on $GdScO_3$ (Ba_2RuO_4/GSO). See Figs. 3(a)–3(d) for the associated spectral function of quasiparticles simulating the ARPES data, where the xy band is electronlike in Figs. 3(a) and 3(b) and holelike in Figs. 3(c) and 3(d) [49]. Interestingly, the DFT calculations consistently underestimate the density of states and the Lindhard susceptibility at small $\vec{q}$ of the xy band: $N^{xy}(0)$ and $\Pi^{xy}_{ph}(\vec{q})$ at small $\vec{q}$. For our RG analysis we use the parameters $t_x = t_y \equiv t$, $t^{\perp}_x = t^{\perp}_y \equiv t^{\perp}$, and $t'_x = t'_y \equiv t'$ extracted from the ARPES data of Ref. [34].

In Fig. 4 we show the resulting most negative eigenvalues $\tilde{\lambda}^{\alpha}_{s/t}$ of singlet and triplet channels hosted by each band α for the four representative samples. Since the measured effect of strain on the band structures of the 1D bands is mild, the eigenvalues associated with the 1D bands do not change drastically. The tight competition between different channels of the unstrained system [31,36] is lifted as the triplet pairing tendency of the 2D band shoots up to become the clearly leading instability in the vicinity of the Lifshitz transition. Moreover, this leading pairing tendency shows a striking nonmonotonic dependence on the strain with a significantly improved pairing tendency in film Ba_2RuO_4/STO. Importantly, as the Ba_2RuO_4/STO film is slightly away from the actual van Hove singularity by a short distance δ [see Fig. 3(c)] triplet pairing is allowed by symmetry.

The significant enhancement in the triplet pairing tendency of the 2D band in the Ba_2RuO_4/STO film is due to the conspiracy between the enhanced DOS of the 2D band and the associated enhancement in the ferromagnetic fluctuation in the measured band structure that enters the triplet pairing vertex through the bare particle-hole bubble $\Pi^{xy}_{ph}(\vec{q} = 0)$. Interestingly, although the singlet pairing tendency of the 2D

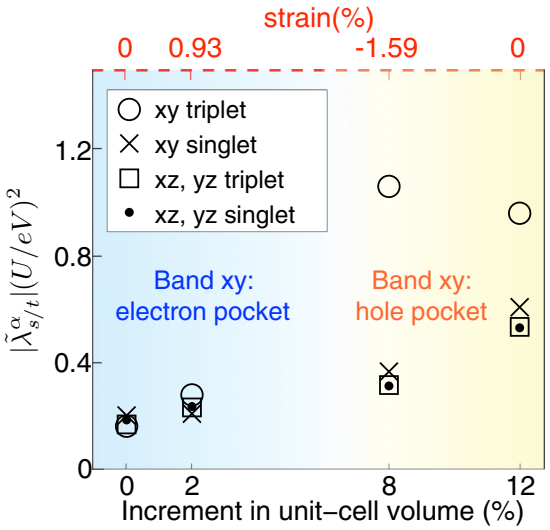

FIG. 4. The magnitudes of the most negative eigenvalues $\tilde{\lambda}^{\alpha}_{s/t}$ of different channels $(\alpha,s/t)$ for the four representative samples. In the order of increasing volume of one unit cell, the ticks on the horizontal axis mark the four representative samples: the bulk Sr_2RuO_4 (0%), and the films Sr_2RuO_4/STO(2%), Ba_2RuO_4/STO(8%), and Ba_2RuO_4/GSO(12%). The percentage refers to the increase in the volume of one unit cell compared to that of the unstrained bulk Sr_2RuO_4. The upper horizontal axis shows the in-plane strain of each Sr_2RuO_4 and Ba_2RuO_4 sample defined with respect to the bulk Sr_2RuO_4 and Ba_2RuO_4/GSO, respectively.

band also benefits from the enhanced DOS of the 2D FS near the van Hove singularity, the antiferromagnetic fluctuation which facilitates the singlet pairing does not benefit from the proximate van Hove singularities as much due to the lack of perfect nesting.

V. SUMMARY

To summarize, we theoretically investigated how strain-driven changes in band structure should impact the superconducting instabilities in ruthenates. Considering the effect of mild uniaxial strain of the degree achieved in Ref. [20], we confirmed our approach of using the strained band structure as an input to the RG calculation to qualitatively reproduce the observed T_c dependence on the lattice strain. We then noted by order of a few % strain that the FSs can be altered sufficiently to come close to the nearby van Hove singularity. As such a degree of biaxial strain has been achieved by some of us [34] and shown to result in van Hove singularity in the 2D band, we used the band structure extracted from ARPES data as the input to the weak-coupling RG procedure and predicted triplet superconductivity with enhanced T_c to be driven predominantly by 2D bands near van Hove singularity. In order to test our predictions, the film purity [14] and structural order [50,51] need to improve. Recent success in growing superconducting Sr_2RuO_4 thin films [52] makes us optimistic that point defects and extended defects of strained films can be sufficiently reduced.

It is important to note that in the proposed strategy of engineering FSs and using the resulting band structure as an input to an RG procedure, the aspects of results that are of great interest, such as the dominant pairing channel and the T_c, are nonuniversal aspects that are sensitive to microscopic details. As we propose to use this very sensitivity to engineer a desired superconductor with the advancement of experimental capabilities [20,34,53], we should also stress the importance of basing the microscopic model on the measurement of the actual band structure.

Note added. Recently, we have become aware of two preprints Refs. [48,53] focusing on the uniaxial strain effects on Sr_2RuO_4. Steppke *et al.* [53] experimentally achieved the necessary uniaxial strain to access the van Hove singularity and compared the results with a theoretical approach similar to that used in this paper but with a somewhat different microscopic model. Liu *et al.* [48] used a functional renormalization-group approach on a single band model focusing on the 2D band to study the competition between superconductivity and spin-density waves under uniaxial strain approaching van Hove singularity.

ACKNOWLEDGMENTS

The authors are grateful to A. Mulder, S. Raghu, A. Chubukov, A. MacKenzie, T. Scaffidi, F. Zhang, S. Kivelson, R. Thomale, and H. Yao for helpful discussions. This work was supported by the Cornell Center for Materials Research with funding from the NSF MRSEC program (Grant No. DMR-1120296). Y.-T.H. and E.-A.K. acknowledge support from NSF Grant No. DMR-0955822. W.C. was supported by NSF Grant No. DMR-1265593. A.F.R. and C.J.F. acknowledge support from the NSF Grant No. DMR-1056441.

APPENDIX A: EFFECTS OF STRAIN ON BANDWIDTH AND OCCUPATION

When either uniaxial or biaxial tensile strain is applied to the ruthenates, the bond length along the direction of strain increases which causes band flattenings in the same direction (see Fig. 1 of the main text). On the other hand, a dramatic change in the shape of the bands is at the same time accompanied by a charge transfer among different bands. In Fig. 5 we show the d-orbital crystal-field splitting corresponding to the RuO_6 octahedra in Sr_2RuO_4 before and after applying strain (for comparison we also include the splitting corresponding to a perfect octahedral environment). In the biaxial case, tensile strain enlarges both in-plane lattice parameters while simultaneously reducing the out-of-plane one. The resulting octahedron is then less elongated, and the energy splitting between orbital xy and orbital xz,yz is reduced. Consequently the occupation of the xy level increases. Such charge transfer together with the flattening of the xy band along the strain direction could bring the quasi-2D Fermi surface which is already close to van Hove singularity in the absence of strain to one or both of the van Hove points $X=(\pi,0)$ and $Y=(0,\pi)$. Similar effects occur in Ba_2RuO_4 under an opposite direction of strain due to the fact that the Fermi level lies above the van Hove points instead of below (see Fig. 1 of the main text).

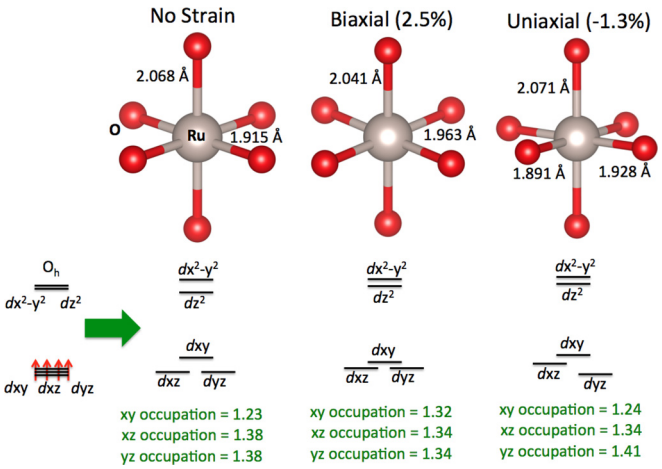

FIG. 5. Crystal-field splitting of energy levels in Sr_2RuO_4: unstrained, under tensile biaxial strain and under compressive [100] uniaxial strain. Octahedral symmetry is broken in the three cases. In the biaxial case, changes in the bond lengths decrease the energy difference between xy and xz, yz levels, increasing the xy occupation. For the uniaxial case, bond lengths are reduced along the [100] direction and increased along [010], and as a result the xz and yz levels are shifted up and down, respectively.

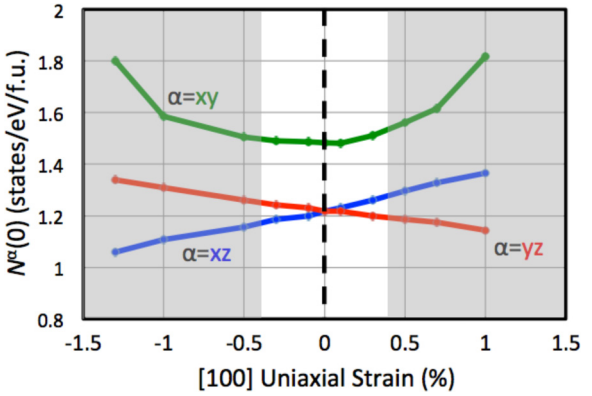

FIG. 6. The density of states at the Fermi level for xz, yz, and yz bands under tensile (>0) and compressive (<0) uniaxial strain. The unshaded regime is the regime with small strain magnitude which corresponds to Fig. 2(b) in the main text.

APPENDIX B: DFT CALCULATION ON STRAINED RUTHENATES

In order to gain a deeper insight into the interplay between strain and electronic structure in ruthenates we perform DFT calculations by systematically varying the applied amount of uniaxial and biaxial strain. We use the PBEsol exchange-correlation functional as implemented in VASP [54,55] with a plane-wave basis cutoff of 520 eV. For structural and static calculations we use $8 \times 8 \times 4$ and $12 \times 12 \times 12$ samplings, respectively, of the Brillouin zone. Full structural relaxations are performed on Ba_2RuO_4 and Sr_2RuO_4, and the optimized cells thus obtained are the unstrained unit cells we later use in uniaxial and biaxial calculations. The resulting lattice constants are in both cases in good agreement with experiment: The obtained values are $a = 3.947$ Å (expt. 3.990 Å), $c = 13.417$ Å(expt. 13.430 Å) for Ba_2RuO_4 and $a = 3.831$ Å (expt. 3.871 Å), $c = 12.731$ Å (expt. 12.739 Å) for Sr_2RuO_4 [34]. Despite the negligible underestimation of the experimental value for the c lattice constant, we find the calculated in-plane lattice constant a to be underestimated by 1% for both ruthenates, which leads to an artificial elongation in the RuO_6 octahedron. Moreover, although the Fermi velocities of all three bands xz, yz, and xy are underestimated compared to the ARPES data, in particular, we find the Fermi velocity of band xy to be underestimated the most which agrees with the observation made in Ref. [34]. These underestimations in turn reduce the xy band occupations and the DOS at the Fermi level for this band.

1. Uniaxial strain

We relax the internal structural degrees of freedom and transverse lattice constants by keeping the [100] direction fixed at the desired strain amount. The FSs and dispersions obtained from DFT are then used to fit the parameters for the tight-binding model in Eq. (2) in the main text.

In Fig. 6 we show the evolution of the band-projected DOS at Fermi level $[N^\alpha(0)]$ as a function of the [100] uniaxial strain in Sr_2RuO_4. As bond lengths along the x direction are reduced, bond lengths along y increase. Consequently yz bands become less dispersive, and the number of states at the Fermi level is increased while it is reduced for xz. At the same time occupation for the xz bands decreases, whereas increasing for yz (see Fig. 5). Note that although the DOS of the xy band starts to thrive at a large amount of strain due to the van Hove singularity, the growths in the DOS of the $xz(yz)$ and xy bands under a small amount of tensile(compressive) strain are of similar magnitudes as shown in the unshaded area. This small strain regime is the regime where we investigate the superconducting tendencies in Fig. 2(b) of the main text.

In our calculation, the xy band meets the van Hove points X and Y at the Fermi level for a [100] compressive strain of

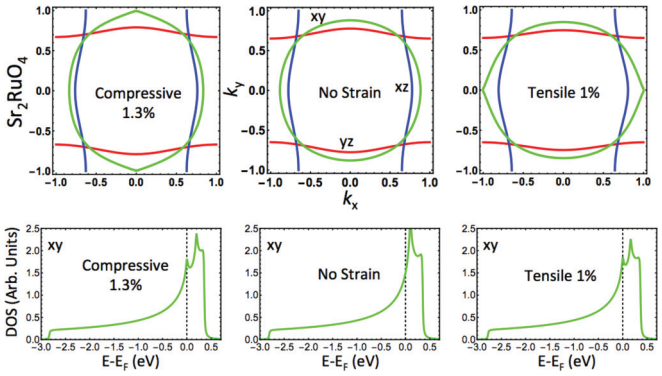

FIG. 7. FSs at $k_z = 0$ for Sr_2RuO_4 (top panel) and the corresponding DOS for the xy band (bottom panel) as a function of the [100] uniaxial strain. The uniaxial strain lowers the symmetry from D_{4h} to D_{2h}. As a result, whereas the peak in the DOS of the xy band due to the van Hove point $X = (\pi,0)$ sits at the Fermi level, the peak due to the van Hove point $Y = (0,\pi)$ lies above the Fermi level by around 200 meV. Units of k_x and k_y are π/a and π/b, respectively, where a and b are the in-plane lattice constants.

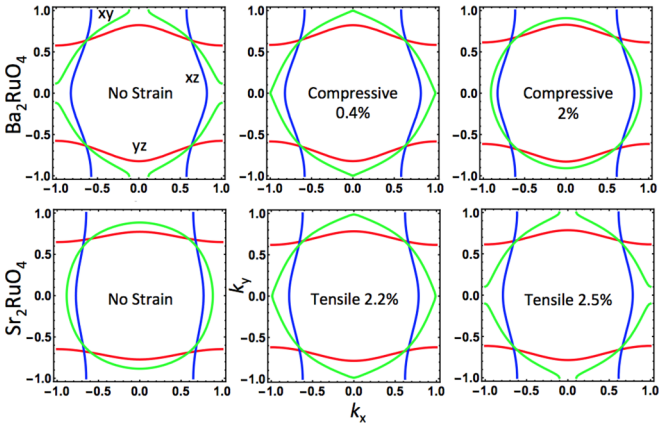

FIG. 8. FSs at $k_z = 0$ for Ba_2RuO_4 (top panel) and Sr_2RuO_4 (bottom panel) as a function of strain obtained by fitting the tight-binding model to DFT data. Although the Fermi level of Sr_2RuO_4 approaches the van Hove points $X = (\pi,0)$ and $Y = (0,\pi)$ under a tensile strain, the opposite trend is predicted for Ba_2RuO_4. k_x and k_y are in units of π/a where a is the in-plane lattice constant.

1.3% and for a [100] tensile strain of 1% (see the top panel of Fig. 7). The larger value for the [100] compressive strain is due to the in-plane Poisson ratio (≈0.4) [56] of Sr_2RuO_4. From the xy band DOS shown in the bottom panel of Fig. 7, we notice the peak due to van Hove singularities in the unstrained case splits into two peaks under strain. This is a consequence of uniaxial strain reducing the symmetry from D_{4h} to D_{2h}.

2. Biaxial strain

We perform DFT calculations for a wide range of values of tensile and compressive strain by fixing the in-plane lattice constants and letting all internal and out-of-plane lattice constant relax. We then fit the tight-binding model presented in the main text to our DFT data. As illustrated in Fig. 1 in the main text, in the case of Sr_2RuO_4 the hopping parameters decrease, and the bands become flatter with tensile strain, thus approaching the van Hove singularity. Due to the simultaneous increase in in-plane bond lengths together with a decrease in the out-of-plane ones, xy energy levels move downwards whereas xz and yz are shifted up (Fig. 5). As mentioned in Sec. I, this results in an enhancement of the xy occupation which further contributes to reaching the van Hove singularity. Our calculations predict a peak in the DOS of the xy band due to the Van Hove singularities at both X and Y at the Fermi level for a tensile strain of ≈2.2% (lower panels in Figs. 8 and 9). Contrarily, for Ba_2RuO_4 it requires a compressive strain of ≈0.4% (upper panel in Fig. 8). This is due to the fact that in Ba_2RuO_4 the xy band lies below the Fermi level and thus a compressive strain needs to be applied in order to increase the hopping parameters and broaden the band (see Fig. 1 in the main text). One important difference from the uniaxial strain case is that D_{4h} symmetry is preserved under biaxial strain such that the xy band FS can meet both van Hove points simultaneously. Thus the DOS of the xy band only has a single peak due to the van Hove singularity with a much higher intensity (see Fig. 9) than the small split peak at the Fermi level of uniaxially strained Sr_2RuO_4 (see the bottom panel of Fig. 7).

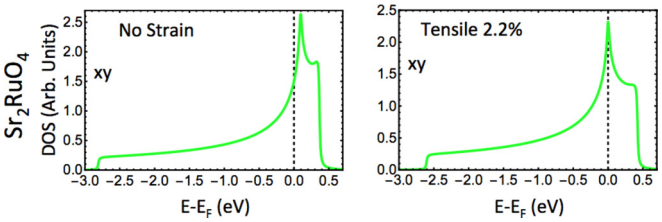

FIG. 9. The density of states for Sr_2RuO_4 before and after applying the biaxial strain.

[1] G. Volovik, JETP Lett. **66**, 522 (1997).
[2] N. Read and D. Green, Phys. Rev. B **61**, 10267 (2000).
[3] D. A. Ivanov, Phys. Rev. Lett. **86**, 268 (2001).
[4] S. Das Sarma, C. Nayak, and S. Tewari, Phys. Rev. B **73**, 220502 (2006).
[5] C. Nayak, S. H. Simon, A. Stern, M. Freedman, and S. Das Sarma, Rev. Mod. Phys. **80**, 1083 (2008).
[6] M. Stone and R. Roy, Phys. Rev. B **69**, 184511 (2004).
[7] S. B. Chung, H. Bluhm, and E.-A. Kim, Phys. Rev. Lett. **99**, 197002 (2007).
[8] K. Ishida, H. Mukuda, Y. Kitaoka, K. Asayama, Z. Q. Mao, Y. Mori, and Y. Maeno, Nature (London) **396**, 658 (1998).
[9] K. D. Nelson, Z. Q. Mao, Y. Maeno, and Y. Liu, Science **306**, 1151 (2004).
[10] F. Kidwingira, J. D. Strand, D. J. Van Harlingen, and Y. Maeno, Science **314**, 1267 (2006).
[11] J. R. Kirtley, C. Kallin, C. W. Hicks, E.-A. Kim, Y. Liu, K. A. Moler, Y. Maeno, and K. D. Nelson, Phys. Rev. B **76**, 014526 (2007).
[12] P. J. Curran, S. J. Bending, W. M. Desoky, A. S. Gibbs, S. L. Lee, and A. P. Mackenzie, Phys. Rev. B **89**, 144504 (2014).
[13] J. Jang, D. G. Ferguson, V. Vakaryuk, R. Budakian, S. B. Chung, P. M. Goldbart, and Y. Maeno, Science **331**, 186 (2011).
[14] A. P. Mackenzie, R. K. W. Haselwimmer, A. W. Tyler, G. G. Lonzarich, Y. Mori, S. Nishizaki, and Y. Maeno, Phys. Rev. Lett. **80**, 161 (1998).
[15] Y. Maeno, T. Ando, Y. Mori, E. Ohmichi, S. Ikeda, S. NishiZaki, and S. Nakatsuji, Phys. Rev. Lett. **81**, 3765 (1998).
[16] C. Autieri, M. Cuoco, and C. Noce, Phys. Rev. B **85**, 075126 (2012).
[17] Y. A. Ying, N. E. Staley, Y. Xin, K. Sun, X. Cai, D. Fobes, T. J. Liu, Z. Q. Mao, and Y. Liu, Nat. Commun. **4**, 2596 (2013).
[18] S. Kittaka, H. Yaguchi, and Y. Maeno, J. Phys. Soc. Jpn. **78**, 103705 (2009).
[19] S. Kittaka, H. Taniguchi, S. Yonezawa, H. Yaguchi, and Y. Maeno, Phys. Rev. B **81**, 180510 (2010).
[20] C. W. Hicks, D. O. Brodsky, E. A. Yelland, A. S. Gibbs, J. A. N. Bruin, M. E. Barber, S. D. Edkins, K. Nishimura, S. Yonezawa, Y. Maeno, and A. P. Mackenzie, Science **344**, 283 (2014).

[21] W. Kohn and J. M. Luttinger, Phys. Rev. Lett. **15**, 524 (1965).
[22] D. Zanchi and H. J. Schulz, Phys. Rev. B **54**, 9509 (1996).
[23] C. J. Halboth and W. Metzner, Phys. Rev. B **61**, 7364 (2000).
[24] M. Salmhofer, Commun. Math. Phys. **194**, 249 (1998).
[25] C. Honerkamp, M. Salmhofer, N. Furukawa, and T. M. Rice, Phys. Rev. B **63**, 035109 (2001).
[26] S. Raghu, S. A. Kivelson, and D. J. Scalapino, Phys. Rev. B **81**, 224505 (2010).
[27] H. Zhai, F. Wang, and D.-H. Lee, Phys. Rev. B **80**, 064517 (2009).
[28] R. Thomale, C. Platt, J. Hu, C. Honerkamp, and B. A. Bernevig, Phys. Rev. B **80**, 180505 (2009).
[29] A. V. Chubukov, D. V. Efremov, and I. Eremin, Phys. Rev. B **78**, 134512 (2008).
[30] R. Nandkishore, L. S. Levitov, and A. V. Chubukov, Nat. Phys. **8**, 158 (2012).
[31] S. Raghu, A. Kapitulnik, and S. A. Kivelson, Phys. Rev. Lett. **105**, 136401 (2010).
[32] J.-H. Chu, H.-H. Kuo, J. G. Analytis, and I. R. Fisher, Science **337**, 710 (2012).
[33] C. W. Hicks, M. E. Barber, S. D. Edkins, D. O. Brodsky, and A. P. Mackenzie, Rev. Sci. Instrum. **85**, 065003 (2014).
[34] B. Burganov, C. Adamo, A. Mulder, M. Uchida, P. D. C. King, J. W. Harter, D. E. Shai, A. S. Gibbs, A. P. Mackenzie, R. Uecker, M. Bruetzam, M. R. Beasley, C. J. Fennie, D. G. Schlom, and K. M. Shen, Phys. Rev. Lett. **116**, 197003 (2016).
[35] We are not including the interorbital repulsion V in this paper. Nevertheless we have checked that the interorbital $V \leqslant 0.5U$ makes no qualitative difference to the results we report.
[36] T. Scaffidi, J. C. Romers, and S. H. Simon, Phys. Rev. B **89**, 220510 (2014).
[37] E. J. Rozbicki, J. F. Annett, J.-R. Souquet, and A. P. Mackenzie, J. Phys.: Condens. Matter **23**, 094201 (2011).
[38] C. Kallin, Rep. Prog. Phys. **75**, 042501 (2012).
[39] M. W. Haverkort, I. S. Elfimov, L. H. Tjeng, G. A. Sawatzky, and A. Damascelli, Phys. Rev. Lett. **101**, 026406 (2008).
[40] C. N. Veenstra, Z.-H. Zhu, M. Raichle, B. M. Ludbrook, A. Nicolaou, B. Slomski, G. Landolt, S. Kittaka, Y. Maeno, J. H. Dil, I. S. Elfimov, M. W. Haverkort, and A. Damascelli, Phys. Rev. Lett. **112**, 127002 (2014).
[41] M. H. Fischer and E. Berg, Phys. Rev. B **93**, 054501 (2016).
[42] R. Shankar, Rev. Mod. Phys. **66**, 129 (1994).
[43] We should note that the DFT electronic structure significantly underestimates the density of states and the ferromagnetic fluctuation of the 2D band xy in particular, which can affect the balance.
[44] L. Vaugier, H. Jiang, and S. Biermann, Phys. Rev. B **86**, 165105 (2012).
[45] H. Yao and F. Yang, Phys. Rev. B **92**, 035132 (2015).
[46] R. Nandkishore, R. Thomale, and A. V. Chubukov, Phys. Rev. B **89**, 144501 (2014).
[47] M. L. Kiesel, C. Platt, W. Hanke, D. A. Abanin, and R. Thomale, Phys. Rev. B **86**, 020507 (2012).
[48] Y. C. Liu, F. C. Zhang, T. M. Rice, and Q. H. Wang, arXiv:1604.06666.
[49] The simulation included an additional hybridization term between the 1D bands with strength $V_{hyb}(\vec{k}) = 4t_{hyb} \sin k_x \sin k_y$ extracted from the ARPES data [34].
[50] Z. Q. Mao, Y. Mori, and Y. Maeno, Phys. Rev. B **60**, 610 (1999).
[51] M. A. Zurbuchen, Y. Jia, S. Knapp, A. H. Carim, D. G. Schlom, L.-N. Zou, and Y. Liu, Appl. Phys. Lett. **78**, 2351 (2001).
[52] Y. Krockenberger, M. Uchida, K. S. Takahashi, M. Nakamura, M. Kawasaki, and Y. Tokura, Appl. Phys. Lett. **97**, 082502 (2010).
[53] A. Steppke, L. Zhao, M. E. Barber, T. Scaffidi, F. Jerzembeck, H. Rosner, A. S. Gibbs, Y. Maeno, S. H. Simon, A. P. Mackenzie, and C. W. Hicks, arXiv:1604.06669.
[54] G. Kresse and J. Furthmüller, Phys. Rev. B **54**, 11169 (1996).
[55] P. E. Blöchl, Phys. Rev. B **50**, 17953 (1994).
[56] J. Paglione, C. Lupien, W. A. MacFarlane, J. M. Perz, L. Taillefer, Z. Q. Mao, and Y. Maeno, Phys. Rev. B **65**, 220506(R) (2002).